פרויקט מחקר 085852

Characterization of Unsteady Laminar Separation Bubble on Pitching NACA0018

איפיון בועת ניתוק בכנף NACA0018 בעלת עלרוד משתנה

Student:
Naama Aliskevicius
ID: 324230739
naama.ali@campus.technion.ac.il

Supervisor:
Assoc. Prof. Oksana Stalnov
oksana.s@technion.ac.il

Faculty of Aerospace Engineering
January 2, 2024

Abstract

This study explores phenomena occurring in low-Reynolds-number flows over airfoils during pitching motion. Our primary objective is to comprehensively examine the effects of various flow parameters on the progression of a laminar separation bubble (LSB) in terms of its location and velocity along the wing. Additionally, we examine the Kutta condition using three different methods. By comparing the theoretical methods to the experimental ones, we can analyze the accuracy of each method in attached and detached flows. We experimentally investigate the unsteady phenomenon at low Reynolds numbers under periodic pitching motion with a symmetric NACA 0018 airfoil geometry. To examine the role of reduced frequency on the unsteady aerodynamic phenomenon—for example, propagation of the LSB-in terms of its location and velocity along the airfoil. Furthermore, we study the unsteady Kutta condition when the effect of the LSB is eliminated, i.e. with an increased turbulence level, and when a laminar separation bubble is present. The validity of thin airfoil theory and the Kutta condition [1] is examined by comparing the theoretical methods, based on circulation and thin airfoil theory, to the experimentally measured values [1–3]. The results indicate that the reduced frequency has no influence on the location of the laminar separation bubble, and by analyzing its velocity, we can determine the minimal and maximal locations of the bubble on the wing. Furthermore, we determined the lift coefficient and circulation using the following methods: (I) Wagner's model, (ii) the Kutta-Joukowski theorem (via the circulation), and (iii) pressure measurements at the trailing edge. The examination of the Kutta condition revealed that in the case of the attached flow, the comparison between the three methods was satisfactory, indicating the validity of the Kutta condition for both Wagner's model and the Kutta-Joukowski theorem. When comparing lift coefficients, in the case of detached flow, there was a significant difference between the pressure measurements and the Kutta-Joukowski theorem, suggesting that the Kutta condition will no longer be valid for any of this methodology. Similarly, when the LSB was present, there was a difference between Wagner's model results and the pressure measurements, indicating that the Kutta condition would be invalid. However, when comparing the trailing edge measurements with the results from the Kutta-Joukowski theorem, good compatibility was observed, suggesting the validity of the Kutta condition when comparing these two methods. This study provides new insights into the influence of reduced frequency on a laminar separation bubble and the unsteady Kutta condition.

1 Background and Introduction

The aerodynamic response due to an airfoil in motion has generated widespread attention for nearly a century [6–8]. This interest in the topic is motivated by the need for an accurate description of unsteady aerodynamic loads, as it is essential in the context of separated flows [9], noise prediction [10–12], and flutter [13]. Many modern problems involve the evaluation of structural nonlinearities that necessitate using time-domain aerodynamic models based on unsteady thin airfoil theory [14].

Unsteady thin airfoil theory and pitching motion constitute a fundamental aerodynamics framework describing the dynamic behavior of aircraft and other objects in fluid flows. Unlike steady-state conditions, where airfoil performance remains constant, unsteady conditions create variations in airflow parameters due to the airfoil's motion. When combined with pitching motion, where an airfoil undergoes cyclic changes in its angle of attack, the complex relationships between aerodynamic forces, inertia, and fluid dynamics become challenging to predict. This dynamic interaction determines the lift, drag, and moment characteristics essential for understanding the maneuverability and stability of aircraft during takeoff, landing, and various flight maneuvers.

Additionally, when an airfoil undergoes cyclic changes in its angle of attack, the fluctuating aerodynamic forces lead to variations in the developed flow field, pressure distribution, and vortices shed from its surface. These dynamic flow phenomena can generate significant noise [15], particularly in flow separation and reattachment regions. The unsteady nature of the pitching motion contributes to noise production, as it introduces periodic fluctuations in the flow that can resonate with the natural frequencies of the airfoil or other components, resulting in tonal noise components.

In this context, exploring the limits of unsteady thin airfoil theory opens new avenues to optimize aircraft performance and reduce noise emissions while enhancing operational capabilities. For this purpose, many studies have aspired to model aerodynamic loads with satisfactory accuracy using theoretical [3, 6], experimental [16, 17], or numerical [18] methods.

Unsteady Thin Airfoil Theory

Unsteady thin airfoil theory is based on the steady one that describes potential flow over an airfoil with no thickness. The unsteady theory introduces more complexity relative to the steady one and requires particular treatment to model the aerodynamic loads. The groundwork for analyzing these cases commenced at the beginning of the 20th century, aiming to find the aerodynamic loads on an airfoil in motion. It is based on the classical thin airfoil theory, where the lift and moment are described by the distribution of vortices along the chord line [19]. The analysis is based on the principle that an airfoil in uniform flow can be replaced by a vortex sheet along the chord line, and the strength of this sheet is determined by the condition that the camber line is streamlined. To uphold this assumption, the aggregate of all velocity components normal to the mean camber line must be zero.

In modern aerodynamics, analytical theories for unsteady flow with small disturbances are derived under the assumptions of a flat plate (thin airfoil) in inviscid, incompressible, irrotational, and two-dimensional flow with a planar wake. These assumptions can be the leading cause for the incompatibility between the theoretical model and the experimental results, especially for unsteady aerodynamics. The cornerstone models for unsteady aerodynamics were developed by Wagner [3] in the time domain and by Theodorsen [6] in the frequency domain.

Wagner described lift generation on an airfoil as a function of the angle of attack in arbitrary motion. The lift is generated due to circulatory and added mass contributions. The Wagner function describes the circulatory lift component created by the shed vortices' influence on the wake. Following Wagner's work, Theodorsen investigated the aerodynamic loads on a periodically oscillating airfoil. Continuing Theodorsen, Garrick [20] investigated the force by an airfoil undergoing pitching or heaving motions [19, 21], and Sears[22] showed this system could be described as a stationary flat plate interacting with an incompressible gust. With von Kármán [22], they estimated a thin airfoil's aerodynamic loads, momentum, and lift. Later on, Kemp [23] showed that the transfer function between the aerodynamic force and the gust upwash velocity is related to Sears' function for a periodic gust.

The initial experimental efforts were focused on validating these existing theoretical models [3, 6, 22]. Walker [24] conducted an experiment using the RAF 130 airfoil at a Reynolds number of 1.4×10^{-5} that verified some of Wagner's predictions, despite the fact the model is based on inviscid flow. It was shown that Wagner's prediction is valid only for thin airfoils at very small angles of attack due to the assumption that the trailing edge vortex (TEV) sheet is planar. Halfmann [25] found an agreement in the general trend experimentally, but his data differs by about 30% from theoretical values. Keeping the assumption that the TEV sheet is planar, but now looking at a thick airfoil with a finite trailing edge angle, Chow and Huang [26] obtained a short-time approximation of the lift curve that gives a vanishing lift at the initial time for a finite trailing edge angle in contrast to the Wagner solution, which gives a finite initial lift. Graham [27] claimed that the planar sheet assumption is not suitable for short times, and to deal with that, he suggested approximating the TEV to a concentrated vortex to predict the short-time behavior of the lift before the assumption of monotonically increasing lift can be valid (and Wagner's theory can be used). For longer times, Ford and Babinsky [28] compared the bound circulation, predicted by the Wagner model, to measurements of unsteady lift for an accelerating plate and found that the Wagner lift curve can be a first-order approximation of the circulatory part of the lift [29]. Though the Wagner effect considers the discrete vortex simulations by computational fluid dynamics (CFD) and experimental measurements, it lacks a model that unifies the original Wagner theory and the force model that works for relatively large angles of attack.

For Sears' theory, Jackson [30] investigated the three-dimensional unsteady lift on a NACA 0015 airfoil in homogeneous turbulence. The lift measurements at zero angles of attack agreed with the three-dimensional theory. Still, a further comparison to Sears's two-dimensional theory showed it was very inaccurate. Commerford and Carta [31] investigated unsteady pressure on an airfoil immersed in a sinusoidal, two-dimensional gust and also found reasonable agreement with the Sears function only at low angles of attack. Generally, the agreement between the first-order linear theory and experiments is best for small mean angles, moderately reduced frequencies, and low Mach numbers. In the case of a lifting airfoil with a non-zero mean angle of attack, experimentally obtained transfer functions show a different behavior than the one obtained by the first-order approximations [32].

The common notion is that these models provide a sufficient description of the aerodynamic loads as long as the boundary layer remains attached. However, there seems to be a certain amount of scatter in experimental validations in the time and frequency domains [25, 32, 33]. Furthermore, a comparison among the experimental investigation is challenging due to differences in the experimental setups, such as airfoil thickness and camber, type of motion, mean incidence angle, the amplitude of oscillation, the location of the pitching axis, aspect ratio, Reynolds number, and Mach number. Nevertheless, some overall conclusions can be drawn. In none of the experiments does the experimentally derived transfer function match the theoretical transfer function quantitatively in amplitude and phase. Therefore, further development of both theoretical and experimental models is required due to the difference between these theoretical models and experimental results.

The scarcity of experimental data is primarily due to the difficulty of accurately measuring instantaneous aerodynamic loads, particularly when small variations in the angle of attack are considered. From an experimental perspective, the chosen method in this study for measuring aerodynamic loads is by integrating the surface pressure distribution (**?**). In addition to accurately obtaining sectional lift, it introduces the advantage of analyzing local flow properties such as transition, flow separation, and reattachment. Although this alternative allows investigating the unsteady flow field on the airfoil surface, it requires adequate volume within the airfoil, which limits the pressure transducer's amount, type, and position inside the wind tunnel model or the application of surface pressure sensors. Furthermore, amplitude and phase calibration is required to consider the finite length of the pressure tap tubing system.

Even though the flow problem over an oscillating airfoil has been discussed over the years [4, 34, 35], the conditions under which the classical theory can be applied to describe dynamic response and transient aerodynamic loads remain under scientific debate [36, 37]. Furthermore, despite its age and applicability, the Wagner function has not been extensively validated in experiments due to the difficulty of measuring time-resolved instantaneous unsteady pressures. Hence, A primary motivation of the present study is to verify to what extent the linear theory can be adapted to describe aerodynamic loads during transient and non-periodic motion at low and high angles of attack. Specifically, one particular phenomenon of interest is the presence of a laminar separation bubble (LSB).

Laminar Separation Bubble

At low Reynolds numbers and static conditions, the transition from a laminar boundary layer to a turbulent one is associated with the development of the LSB, which is formed when the laminar boundary layer encounters an adverse pressure gradient and ultimately loses its ability to remain attached before the Tollmien–Schlichting instabilities initiate the transition process [38, 39]. At a certain distance downstream of the laminar separation point, the separated laminar shear layer transitions to a turbulent free-shear layer, returning to the surface, thereby defining a turbulent reattachment point and establishing a turbulent boundary layer. The region between the laminar and turbulent reattachment point defines the LSB. Further downstream, and depending on the pressure recovery parameters, the turbulent boundary layer may or may not undergo turbulent separation, ultimately leading to stall. Under periodic motion, the LSB travels in the direction of the wing chord, making its effects on the lift even more difficult to analyze and predict. The ability to predict the LSB's spatial and temporal behavior is crucial to determine the airfoil aerodynamic performance at low Reynolds numbers [40–42].

Extensive research has been conducted to understand the influence of various factors on LSB in steady conditions. For instance, O'Meara and Mueller [43] characterized steady LSB at different angles of attack by studying static pressure distributions obtained from pressure taps. They observed deviations from inviscid solutions due to the presence of the LSB. Another comprehensive study by Burgmann and Schröder [44] explored the impact of parameters such as freestream turbulence (FST) intensity, Reynolds number, and angle of attack on the size and characteristics of LSB through experimental means. They concluded that the angle of attack has a more pronounced influence on the separation point, transition onset, and reattachment point than the Reynolds number. Consequently, the bubble's length and thickness strongly depend on the Reynolds number, and a weaker one depends on the angle of attack. Moreover, they demonstrated the effect of FST on the geometry of the separation bubble. Similarly, Hosseinverdi and Fasel [45] conducted numerical simulations to assess the influence of FST on the Kelvin-Helmholtz instability and, consequently, the transition process.

Unlike the above-mentioned studies, characterizing the unsteady behavior of LSB poses greater challenges and has thus seen limited experimental investigations. Experiments in this domain [17, 46, 47] have primarily revolved around low-frequency pitching-type motions, revealing hysteresis in the bubble's location between pitch-up and pitch-down phases of the motion cycle. Ericsson [48] explained this behavior using the unsteady version of Bernoulli's equation. Recent research has delved into higher-frequency unsteady motions, as explored by Nati [49] and Guerra [50]. Understanding the dynamics of LSB in unsteady conditions remains critical for optimizing airfoil aerodynamics, particularly in low Reynolds number regimes. Researchers continue to explore these phenomena to improve our ability to predict and manage them in practical applications. The LSB can be detected by a negative pressure peak on the suction side, followed by a pressure plateau. From here, one can track the propagation of the bubble and analyze the effect of flow characteristics on its behavior to develop an accurate model that can predict its behavior and help prevent or minimize its effect on the wing.

Kutta Condition

The Kutta condition has been a pervasive auxiliary requirement in the historical development of potential-flow aerodynamics. This condition finalizes the potential-flow framework by determining the circulation around an airfoil and, consequently, the lift force it generates. The Kutta condition has diverse representations, including smooth flow off the trailing edge, the absence of flow around the trailing edge, or the specific placement of the stagnation point right at the trailing edge.

In the context of steady airfoil flow, the Kutta condition asserts that an airfoil's circulation is directly linked to lift generation [51]. It enforces that the rear stagnation point should coincide with the airfoil's trailing edge. This implies several key characteristics: there should be no pressure discontinuity between the upper and lower surfaces at the trailing edge, the velocity at the trailing edge must remain finite, tangential velocities on both the upper and lower surfaces should be equal at the trailing edge, and there should be no vorticity shed behind the airfoil [52]. In the case of unsteady flow, the Kutta condition is not uniquely defined, leading to the emergence of various approaches and models. Giesing's model [53], for instance, suggests that the flow streamlines can be tangential to either the upper or lower surface of the airfoil at the trailing edge. The direction of vorticity after being shed from the airfoil plays a crucial role in determining whether the stagnation streamline follows the contour of the lower surface or becomes tangent to the upper surface at the trailing edge. This fundamental difference between steady and unsteady airfoil flows and the variability in interpreting the Kutta condition highlights the complexity of flow phenomena, especially in scenarios involving high angles of attack and unsteady conditions.

This model encounters difficulties when the unsteady frequency approaches zero because it fails to converge with the classical Kutta condition. Bisplinghoff [13] proposed introducing a pressure jump at the trailing edge to address this issue. By assuming equal pressures on the upper and lower surfaces near the trailing edge, this modification ensures convergence with the classical Kutta condition. Building on this work, Taha and Razaei [21] expanded Theodorsen's theory. They demonstrated that imposing the classical Kutta condition on an unsteady pitching airfoil could lead to inaccurate phase lags in the lift response. Their research revealed that the viscous extension of Theodorsen's theory exhibited significant deviations from the classical results, especially at high reduced frequencies and low Reynolds numbers. Instead, it displayed improved agreement with results obtained through unsteady Reynolds-averaged Navier–Stokes simulations on a pitching airfoil. Another approach was proposed by Xia and Mohseni [51]. In their model, they accounted for the shedding and convection of vorticity in the wake using a free-wake model. They employed an unsteady Kutta condition based on a momentum balance near the trailing edge. This dynamically determined the location for vorticity shedding. Compared to computational simulations, their model closely matched the results concerning wake dynamics and unsteady loading on a pitching airfoil. Moreover, numerous experiments have indicated that the classical Kutta condition does not hold in unsteady flows [52]. During the 1970s and 1980s, there was an ongoing debate regarding the precise characteristics of the Kutta condition in unsteady flows [54, 55].

A consensus emerged, suggesting that the classical Kutta condition was satisfied in experiments characterized by low-frequency, low-amplitude, and high Reynolds numbers [9]. These specific conditions align with the parameters used in the experiments conducted in this project. By analyzing pressure distributions along the wing, extracting vorticity at the trailing edge and along the wing, and subsequently comparing these results to one another as well as to Wagner's model, we can gain valuable insights into the applicability of the unsteady Kutta condition in both theoretical and experimental contexts.

Motivation

The motivation behind this study arises from the need for a deeper understanding of the phenomena occurring in low-Reynolds-number flows over airfoils. Our primary objective is to comprehensively examine the effects of different flow parameters on the progression of the LSB in terms of its location and velocity along the wing. Additionally, we examine the Kutta condition using three different methods to calculate it. By comparing the theoretical methods to the experimental ones, we can analyze the accuracy of each method in attached and detached flows. This document proceeds as follows: firstly, the experimental approach is described. Afterwards, the key findings obtained in this research are presented and discussed.

The methodology of investigating the LSB is divided into two components. Initially, the flow characteristics' influence on the LSB's behaviour is examined in terms of the location and velocity of the bubble. By identifying significant negative pressure peaks in the instantaneous pressure measurements, the location and velocity of the bubble are evaluated and compared for a range of flow characteristics. The objective is to discern the influence of each characteristic, enabling us to predict aerodynamic loads on the wing. This understanding serves as a foundation for enhancing the overall performance of the wing.

The second part examines the effect of flow separation on validating the unsteady Kutta condition [1]. A unique data set of instantaneous pressure measurements along the wing and on the trailing edge was used to calculate the circulation derivative. Then, using the derivative calculated from the measured pressure on the trailing edge and comparing it to the derivative calculated using Wagner's model [3] and the Kutta-Joukowski theorem [1, 2]. This comparison can reveal a fundamental understanding of what models are more accurate in estimating the aerodynamic loads. In the future, one can locate the main inaccuracies of these theoretical models. These inaccuracies, in which the unsteady Kutta condition fails, can be used to suggest an empirical model that considers the unsteady Kutta condition. The new model can be used in various experiments aspiring to improve manoeuvrability during flight.

2 Review of Mathematical Formulation

The Laplace equation describes Incompressible irrotational flow, a linear equation admitting superposition. Therefore, it is the basis for almost all analytical theories of aerodynamics in the linear regime (such as Wagner's model [3]). However, the use of potential flow isn't comprehensive and needs additional conditions, for instance, the Kutta condition, to provide a complete description. In particular, it does not quantify the vorticity shed at the sharp trailing edge. This quantity is essential as it immediately determines the circulation over the airfoil through the conservation of circulation, which in turn influences the lift via the Kutta-Joukowsky lift theorem [1, 2]. Therefore, the potential flow theory alone cannot predict the generated lift force. However, suppose the generated lift force supplies the potential flow theory. In that case, it will reasonably represent the flow field even in unsteady high angles of attack situations, as examined in this paper.

In this part, we analyse the fulfilment of the unsteady Kutta condition under periodic motion. The first part of this study focuses on the estimation of the lift coefficients using the following approaches: (i) prediction with the thin airfoil theory in the time domain (the Wagner function), (ii) the Kutta-Joukowski's theorem, and (ii) the lift coefficient was measured using instantaneous pressure measurements.

2.1 Integral Parameters

2.1.1 Wagner Model

Wagner [3] has formulated the indicial response function $\phi(\tau)$ of an airfoil due to an abrupt change in the angle of attack. The generation of circulatory lift for an arbitrary motion of a thin airfoil is evaluated by applying Duhamel's superposition integral of indicial step responses, making Wagner's theory useful for describing dynamic response during arbitrary maneuvers (**?**). Under the small-angle of attack assumption, the total lift is a combination of the circulatory and non-circulatory components (also called added mass, apparent mass, or virtual mass) in literature.

For pure pitching motion, the non-circulatory response in the time domain reduces to

$$C_l^{NC}(\tau) = \pi \left(\frac{d\alpha}{d\tau} - a\frac{d^2\alpha}{d\tau^2} \right) \tag{1}$$

where $\dot{\alpha}$ and $\ddot{\alpha}$ are the angular velocity and acceleration, respectively. The no-circulatory response is instantaneous. The circulatory component around the mean angle of attack is achieved mathematically with a Duhamel superposition integral

$$C_l^C(\tau) = \frac{\partial C_l}{\partial \alpha} \left(\alpha_{3/4}(0) + \int_0^\tau \frac{d\alpha_{3/4}}{d\sigma} \phi(\tau - \sigma) d\sigma \right) \tag{2}$$

and combining equations 2,1 we obtain the total lift:

$$C_l^W(\tau) = \pi \left(\frac{d\alpha}{d\tau} - a\frac{d^2\alpha}{d\tau^2} \right) + \frac{\partial C_l}{\partial \alpha} \left(\alpha_{3/4}(0) + \int_0^\tau \frac{d\alpha_{3/4}}{d\sigma} \phi(\tau - \sigma) d\sigma \right) \tag{3}$$

where $\alpha_{3/4}$ is the induced angle of attack at three-quarters chord, $\phi(\tau)$ is the first-order Wagner function, and $\tau = U_\infty t/b$ is the non-dimensional convective time, expressed in semi-chords $b = c/2$. The induced three-quarter-chord angle of attack is related to the instantaneous geometric angle of attack by

$$\alpha_{3/4}(\tau) = \alpha(\tau) + \left(\frac{1}{2} - a\right)\frac{d\alpha}{d\tau} \tag{4}$$

where a is the location of the pitching axis, measured from the mid-chord and normalized by the semi-chord. For pitching motion about the quarter-chord axis, it corresponds to $a = -1/2$. The indicial response function $\phi(\tau)$ is the ratio between the time-dependent lift, obtained by a step change in the angle of attack, and the steady lift, obtained from positioning the airfoil at the same angle of attack.

Although the Wagner function $\phi(\tau)$ is known exactly, it is not formulated in simple analytical terms since rendering Duhamel's integration rather complex. The Wagner function is particularly difficult to compute, with definitions requiring the inverse Laplace or Fourier transform of the Theodorsen function, which is represented using Hankel functions [56]. The lack of a convenient and readily usable expression for the Wagner function has resulted in the formulation of various simplifying approximations that can be used to obviate the problem [56–59]. One of the earliest and perhaps most commonly used Wagner's response function was approximated by Jones [57]

$$\phi(\tau) \approx 1.0 - 0.165e^{-0.0455\tau} - 0.335e^{-0.3\tau} \tag{5}$$

where the lift at the initial instant of motion equals one-half of the final steady-state value. The approximation suggests an exponential decay of the transient circulatory lift response.

2.1.2 Kutta-Joukowski Theorem

The Kutta-Joukowski theorem [1, 2] states that lift per unit span on a two-dimensional body is directly proportional to the circulation around the body [60]. The main assumption in this theorem is potential flow and small angles of attack. The definition for lift per unit span

$$L' = \rho U_\infty \Gamma \tag{6}$$

so the lift coefficient takes the form

$$C_l^{KJ} = \frac{\Gamma}{0.5U_\infty c} \tag{7}$$

where c is the chord length, and Γ is the circulation around the airfoil, defined as:

$$\Gamma(t) = \int_{le}^{te} \gamma(x,t)dx \Rightarrow \dot{\Gamma}^{KJ} = \frac{\partial}{\partial t}\int_{le}^{te} \gamma(x,t)dx \tag{8}$$

where x is the normalized chord coordinates and γ is a single vortex and is defined by the difference between the velocities above and below the wing at a certain point. The mathematical description is according to the following definition

$$\gamma = u_{upper} - u_{lower} \tag{9}$$

where the local velocity u is found directly from the definition of the static pressure coefficient

$$C_p = 1 - \left(\frac{u}{U_\infty}\right)^2. \tag{10}$$

Herein C_l^{KJ} can be calculated and compared to C_l^W.

2.1.3 Experimentally Measured Lift

From the experiment, we obtain the instantaneous pressure coefficient; hence, we can calculate the lift coefficient using the following definition:

$$C_l^M = \oint -C_p d\bar{x} \tag{11}$$

where $d\bar{x} = dx\cos\alpha + dy\sin\alpha$ is the parallel location to the chord. The integration path is clockwise. The definition of the pressure coefficient is according to

$$C_p = \frac{p - p_\infty}{0.5\rho U_\infty^2} \tag{12}$$

where $p(t)$ is the instantaneous local static pressure, p_∞ is the ambient static pressure, U_∞ is the free-stream velocity, and ρ is the density of the air. By converting the differential integral in equation 11 into a summation integral with a finite number of pressure coefficients and locations, the lift coefficient was calculated using trapezoidal rule approximation:

$$C_l^M = \left(\sum_{n=1}^{N} -\frac{C_{p(n+1)} + C_{p(n)}}{2}(x_{n+1} - x_n)\right)\cos\alpha - \left(\sum_{n=1}^{N} \frac{C_{p(n+1)} + C_{p(n)}}{2}(y_{n+1} - y_n)\right)\sin\alpha \tag{13}$$

where N is the number of chordwise pressure taps.

2.2 Unsteady Kutta Condition

The Kutta condition at the sharp trailing edge can be stated in several ways [61, 62]. For example, the pressure must be continuous at the trailing edge (TE):

$$\lim_{y\to 0^+} P(TE, y) = \lim_{y\to 0^-} P(TE, y) \tag{14}$$

where $P(TE)$ represents the pressure near the trailing edge station, and y is the coordinate perpendicular to the chord, 0 is at the height of the leading edge. For potential flow, this condition (14) results in $P_1 = P_2$, where points 1 and 2 are on the edge of the boundary layer at the trailing edge. The assumption that the pressure is constant along the boundary layer thickness is not necessarily valid in the trailing-edge region. As such, if P_1 is the pressure rise across the boundary layer, then the condition Eq.(14) results in

$$P_1 - \Delta P_1 = P_2 - \Delta P_2 \tag{15}$$

which is the modification of the classical Kutta condition ($P_1 = P_2$) as suggested by Preston [63] and Spence [64]. The unsteady Bernoulli's equation can be used to relate P_1 and P_2 as [13, 65]

$$\frac{P_1}{\rho} + \frac{1}{2}u_1^2 + \frac{\partial \phi_1}{\partial t} = \frac{P_2}{\rho} + \frac{1}{2}u_2^2 + \frac{\partial \phi_2}{\partial t} \tag{16}$$

where u is the potential flow velocity (as defined previously in Eq. 10) at the edge of the boundary layer and ϕ is the corresponding velocity potential. Combining Eq.(15) and Eq.(16) and realizing that $\phi_1 - \phi_2 = \Gamma$ results in

$$\dot{\Gamma}^{TE} = \frac{1}{2}(u_2^2 - u_1^2) + \frac{\Delta P_2 - \Delta P_1}{\rho}. \tag{17}$$

By combining Eq.(10) with Eq.(17) we obtain the unsteady Kutta condition at the trailing edge

$$\dot{\Gamma}^{TE} = 0.5U_\infty(C_p^u - C_p^l) + \frac{\Delta P_2 - \Delta P_1}{\rho} \tag{18}$$

where C_p^u and C_p^l correspond to the upper and lower static pressure coefficients, respectively. For simplicity later on, let $\dot{\Gamma}_U = 0.5U_\infty(C_p^u - C_p^l)$, $\dot{\Gamma}_P = \frac{\Delta P_2 - \Delta P_1}{\rho}$ and overall $\dot{\Gamma}_{total} = \dot{\Gamma}_U + \dot{\Gamma}_P$. Now, we can calculate the right-hand side of the Eq.(18) using the measured pressure at $x/c = 0.9$ near the trailing edge. The left-hand side of Eq.(18) can be calculated using the instantaneous pressure with Eqs.(8), (9),(10), or by a theoretical method with the Wagner's model and the definition of lift per unit span according to the Kutta-Joukowski theorem as seen in Eqs.(3) and (7). By deriving it concerning time we can obtain

$$\dot{\Gamma}^W = \frac{\partial}{\partial t}\frac{U_\infty C_l^W}{4} \tag{19}$$

where superscript ^{W} indicates estimation according to the Wagner model. Using Eq.(19) and Eq.(8) and placing them in Eq.(18), one can determine the validation of the Kutta condition on the trailing edge.

3 Experimental Setup

Instantaneous aerodynamic loads were measured in a closed-loop wind tunnel at the Wind Tunnel Complex of Technion's Faculty of Aerospace Engineering. The low-speed wind tunnel has a contraction ratio of 5.76, and it incorporates a test section with a cross-section area of 0.5 m by 0.5 m. An axial fan drives the airflow and can generate free-stream velocity up to $U_\infty = 50$ m/s. Measurements were performed at Reynolds numbers in the $1.5 \times 10^5 < Re_c = U_\infty c/\nu < 3 \times 10^5$, where ν is the kinematic viscosity of air. Schematic of the experimental setup is shown in Figure 1. A two-dimensional NACA 0018 airfoil was mounted vertically at the center of the test section. The wind tunnel model with a chord length of $c = 0.25$ m was constructed of lightweight carbon fiber. The gap between the wingtip and the wind tunnel walls was 2.5 mm to minimize the three-dimensional effects. The model moved at different reduced frequencies $0.04 < k = \frac{\omega b}{U_\infty} < 0.12$ where ω is the frequency the wing moves at.

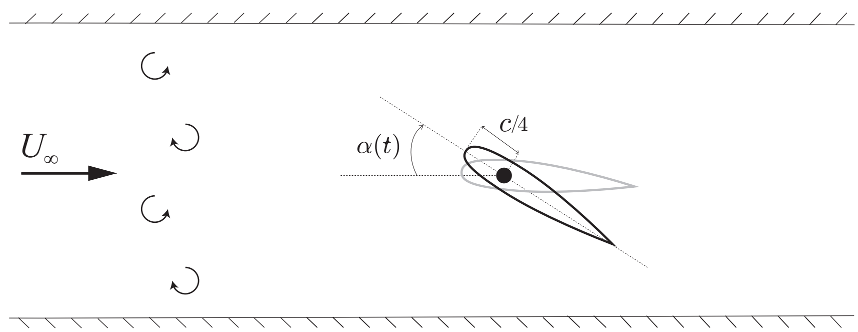

Figure 1: Top view of the experimental set-up. A two-dimensional NACA 0018 airfoil oscillates about the quarter-chord axis in grid-generated turbulence.

A dedicated experimental rig was constructed to generate prescribed periodic motion. The model can be traversed and rotated dynamically by a pair of electromagnetic linear servo motors (Linmot, PS01-37x240F-C), which generate pitching and plunging motion. For simplicity, herein, only pitching motion is considered. The airfoil oscillates around its quarter-chord $x/c = 0.25$ with a mean angle of attack α_m in pitching motion of amplitude α_A. The instantaneous angle of attack is measured with a high-accuracy rotary sensor. All the data were acquired simultaneously with National Instruments (NI) data acquisition PXIe-1082 chassis at a sampling frequency of $F_S = 2$ kHz. Instantaneous pressure, angle of attack, and hot-wire measurements were acquired with 24-bit NI PXIe-4497 cards. The phase and amplitude of a signal were determined by applying the Fast Fourier Transform to each period of the airfoil motion. The analysis of each period independently allows the calculation of the uncertainties in the frequency, magnitude, and phase.

NACA 0018 airfoil geometry was selected mainly due to the availability of an extensive aerodynamic validation database [4, 66, 67]. The airfoil is equipped with 42 pressure taps at the mid-span of the model. Each pressure tap is connected to an HCLA-12X5EB miniature pressure transducer, where all the negative ports of the pressure diaphragm are subject to ambient pressure. Time-resolved lift coefficients were calculated through trapezoidal integration of the chordwise pressure coefficient distribution. To avoid a phase delay, short-length (50 mm) Tygon tubing was used to connect the pressure transducers to the pressure taps. The length of the Tygon tubes was minimized to avoid pressure distortion inside the tubing due to viscous dissipation and resonance [68].

Airfoil aerodynamics at low to moderate Reynolds numbers are characterized by forming a laminar separation bubble, which highly influences the pressure distribution and the corresponding aerodynamic loads. In addition, boundary layer transition introduces a non-linearity to the lift dynamics by generating a significant pressure variation across the boundary layer near the trailing edge, thus affecting the bound circulation around the airfoil [39]. Therefore, the elimination of the laminar separation bubble is of great importance. A passive bi-planar rectangular grid was introduced to elevate the free-stream turbulence intensity above the nominal baseline level (below 0.1%), eliminating the effect of the laminar separation bubble on the aerodynamic loads. The grid was introduced in the contraction section of the wind tunnel, 1.15 m upstream from the airfoil's leading edge. For the characterization of the grid-generated turbulence, measurements of the streamwise velocity in the free stream were performed with one component of hot-wire anemometry. The measured streamwise velocity spectrum is in close agreement with the von-Kármán spectrum for homogeneous and isotropic turbulence with a 2.4% turbulence intensity at $Re_c = 3 \times 10^5$.

Prior to pitching motion analysis, experiments with a static airfoil were performed to determine the airfoil's aerodynamic characteristics. A comparison is made to previously published data by Muller [69]. Figure 2a shows the measured lift coefficient with increased turbulence intensity at $Re_c = 3 \times 10^5$. At low angles of attack, there is no significant variation in static lift coefficient with increasing turbulence level [70]. A marginally higher lift coefficient is generated with lower turbulence intensity at moderate angles of attack. Introducing the passive grid prevents the development of the laminar separation bubble, and delays stall. The corresponding surface pressure coefficient distribution at the studied angles of attack of $\alpha_0 = 3°$ and $\alpha_0 = 6°$ is shown in Figures 2b and Figure 2c. Comparing the chordwise pressure coefficients shows excellent agreement.

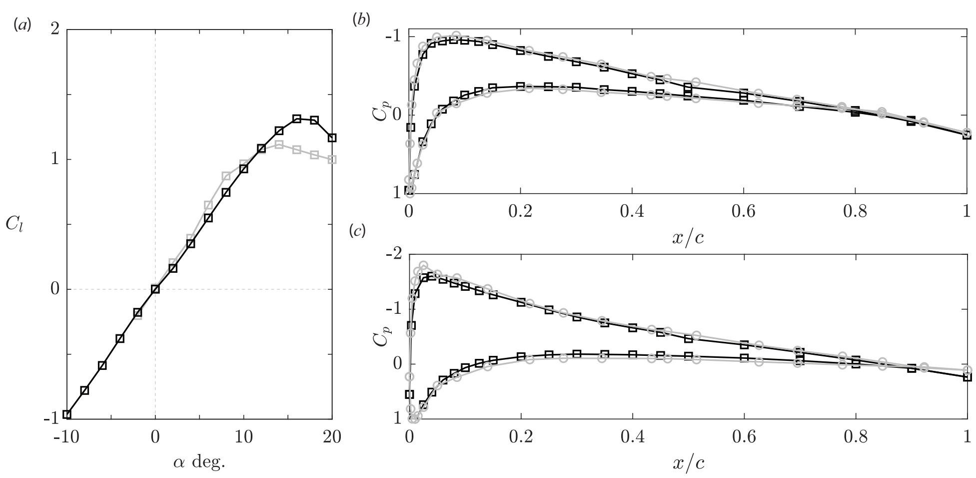

Figure 2: Comparison of the measured (a) lift coefficient and chordwise pressure coefficient distributions at (b) $\alpha_0 = 3°$ and (c) $\alpha_0 = 6°$ at $Re_c = 3 \times 10^5$. Grey markers correspond to data acquired by Muller [69] and black markers to the current experiment with grid-generated turbulence.

4 Results

This study utilizes real-time pressure measurements along the wing to investigate the laminar separation bubble's behaviour and the unsteady Kutta condition in attached, separated, and with an LSB. The analysis was performed by comparing theoretical values to experimental results and analyzing them for all three cases. The pressure measurements were taken as detailed in § 3.

4.1 LSB

This section presents the results of the experimental characterization of the laminar separation bubble under periodic motion. The bubble development within the flow is quantified based on measured instantaneous surface pressure. Figure 3 compares measured static pressure distribution at three typical angles of attack of $\alpha = 6°$, $10°$, and $12°$. The measured static pressure is compared to the one predicted with XFOIL [71]. The mean static pressure distribution confirms the formation of the LSB on the suction side when the airfoil is at positive angles of attack. A pressure plateau is produced after the negative pressure peak on the suction side due to the near-stagnation flow within the laminar separation bubble [72].

The laminar separation bubble is no longer stationary in space when the airfoil is in motion. Figure 4 shows the time history of instantaneous pressure coefficient at two Reynolds numbers, i.e. $Re_c = 2\times10^5$ and $Re_c = 3\times10^5$. The time step of the LSB is evident at multiple locations on the wing. It can be seen that at the lower Reynolds, the LSB is larger in size, and it, therefore, can be more easily detected. Therefore, we focus on $Re_c = 2 \times 10^5$ to determine the algorithm to detect the bubble.

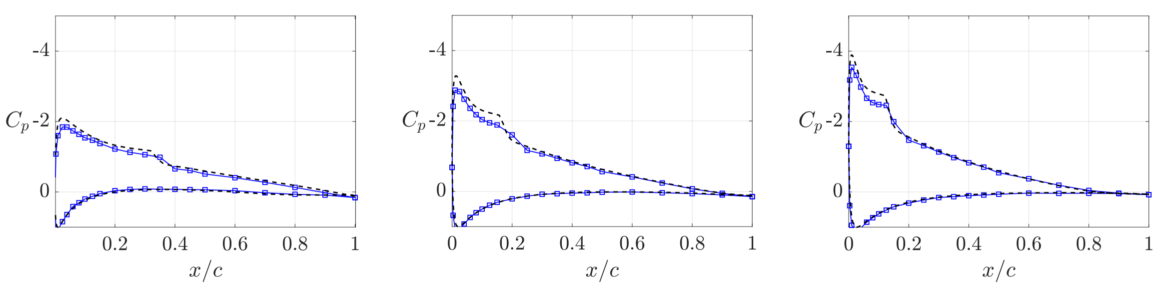

(a) $\alpha_0 = 6°$ (b) $\alpha_0 = 10°$ (c) $\alpha_0 = 12°$

Figure 3: Comparison of the measured static chordwise pressure coefficient distributions at $Re_c = 2 \times 10^5$ and three typical angles of attack.

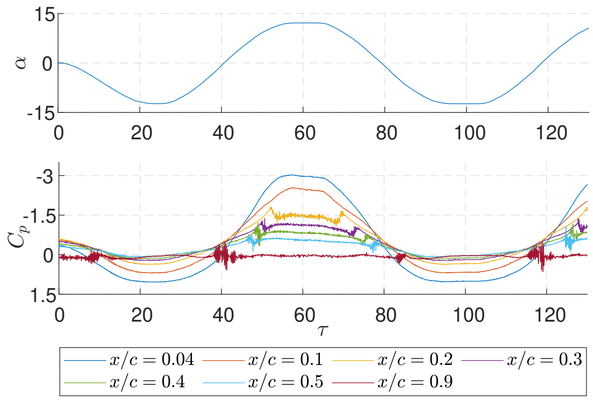

(a) $Re_c = 2 \times 10^5, \alpha = 0 \pm 12°$

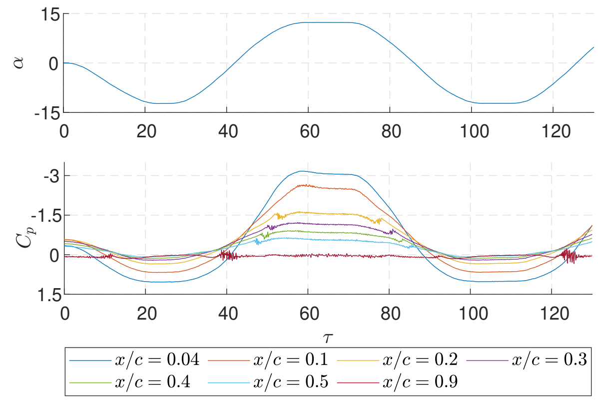

(b) $Re_c = 3 \times 10^5, \alpha = 0 \pm 12°$

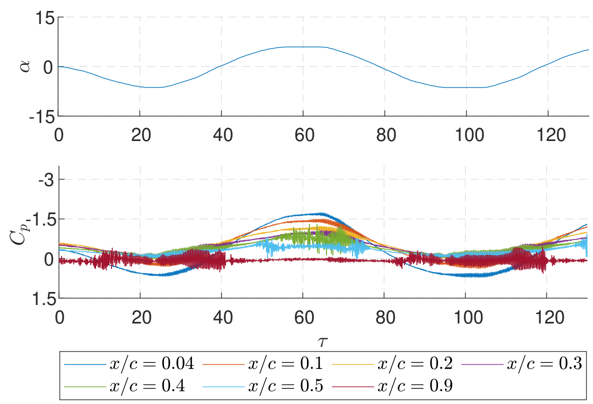

(c) $Re_c = 2 \times 10^5, \alpha = 0 \pm 6°$

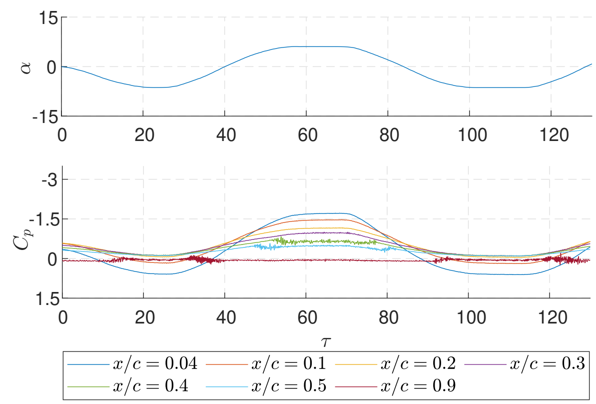

(d) $Re_c = 3 \times 10^5, \alpha = 0 \pm 6°$

Figure 4: Time history of pressure coefficients on the suction surface at various conditions (with a reduced frequency of $k = 0.1$ for all presented cases).

The following methodology was employed in the present study to estimate the LSB's velocity by following the LSB's location through time. The presence of the LSB can be detected by a pressure plateau, as seen in Figure 4, where the LSB is detectable by an unstable flattening of the pressure coefficient instead of a peak. The negative pressure coefficient peak indicates the separation location so it can be tracked by the maximum difference between an estimated "attached" surface pressure (the pressure distribution without an LSB) and the measured surface pressure. The attached surface pressure was estimated using the "smoothdata" Matlab function, using robust quadratic regression. This method is relatively computationally expensive but more robust to outliers.

Figure 5 shows the LSB in numerous cases- for Reynolds number 2×10^5, and initial angle of attack of 6 degrees and an amplitude of 6 degrees, in reduced frequencies of 0.04, 0.06, 0.08, 0.1, 0.12 in laminar flow. In this figure, we can see the location of the LSB along the chord concerning the non-dimensional time. The LSB traveled between $x/c = 0$ to $x/c \approx 0.82$ for all presented reduced frequencies. This means the LSB did not travel to the trailing edge (according

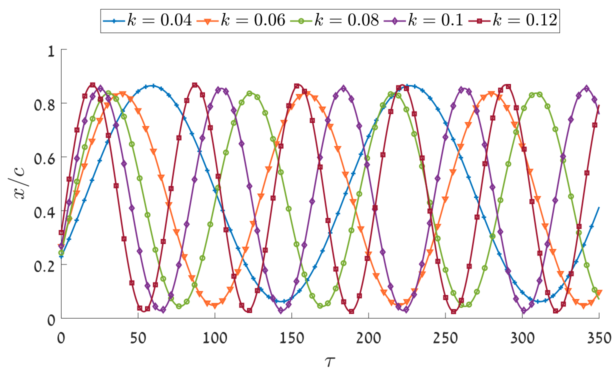

Figure 5: Comparison of the calculated LSB location in different reduced frequencies, at $Re_c = 2 \times 10^5, \alpha = 6^\circ \pm 6^\circ$.

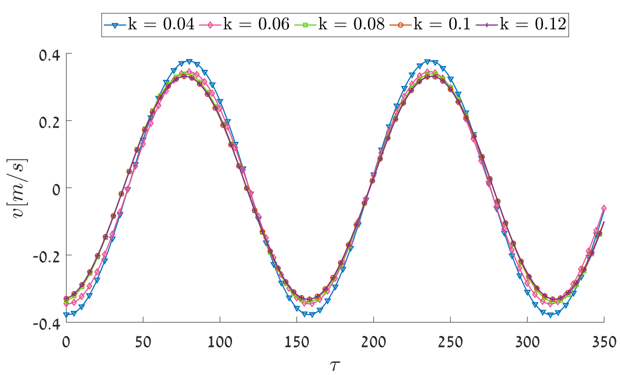

Figure 6: Comparison of the calculated LSB normalized velocity in different reduced frequencies, at $Re_c = 2 \times 10^5, \alpha = 6^\circ \pm 6^\circ$.

to the smoothed results), but by looking at the un-filtered results, a jump in location near the trailing and leading edges appears as noisy and unclear parts of the curve. This forms due to the jump of the LSB as the angle of attack changes from increasing to decreasing. The amplitude for all reduced frequencies tested is almost equal, where the difference between the amplitude is caused by the approximation of the results to a sin function. When looking at the unfiltered results, it is evident that the amplitude of all the curves is equal.

Figure 6 shows the LSB in numerous cases- for Reynolds number 2×10^5, and initial angle of attack of 6 degrees and an amplitude of 6 degrees, in reduced frequencies of 0.04, 0.06, 0.08, 0.1, 0.12 in laminar flow. This figure shows the normalized velocity (normalized by the frequency and ω) concerning the normalized time (τ). We can see that the amplitude for all reduced frequencies is almost the same when the differences stem from the approximation and analysis of the raw data. The amplitude is around 0.4, and we see the amplitude is the same by looking at x/c in the normalized time. Therefore, the minimal and maximal location of the LSB on the wing can be found by normalizing the velocity.

4.2 Kutta condition

In this section, we will discuss the application of Kutta's condition under unsteady motion. Under certain conditions, such as low Reynolds number flows, high-frequency motion of the airfoil, and laminar-to-turbulent transition, the deviation is observed from the classical Kutta condition [62, 73]. It was concluded by Taha and Rezaei [62] that the viscous contributions that are neglected in a potential-flow analysis (employing the Kutta condition at the trailing edge) affect the magnitude of circulation development at lower Reynolds numbers and induce phase shift at higher frequencies. That is, the Kutta condition is one of the reasons behind the inaccurate phase prediction of Theodorsen's lift frequency response function. Before discussing the effect of parameters on the circulation dynamics, let us point out some noteworthy findings.

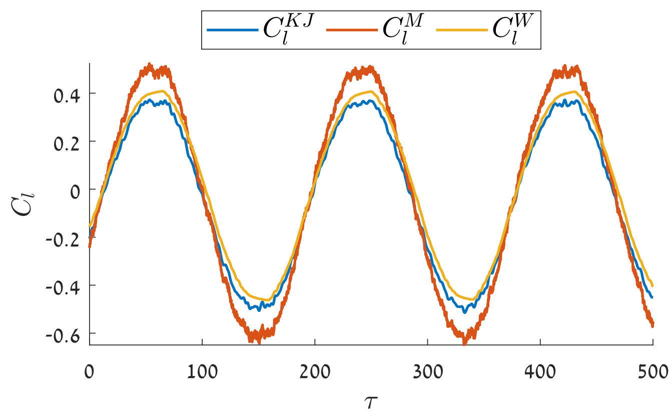

Figure 7: The calculated lift coefficients using Kutta-Joukowski theorem, Wagner's model, and pressure measurements at $Re_c = 3 \times 10^5$, $\alpha = 0° \pm 6°$, $k = 0.04$ with grid-generated turbulence.

Figure 7 compares the calculated lift coefficients using the Kutta-Joukowski theorem, Wagner's model, and pressure measurements for the attached flow. As expected, when the flow is attached, there are small differences between the theoretically calculated $C_l(C_l^{KJ}, C_l^{W})$ and the one estimated from the pressure measurements (C_l^{M}). The difference between C_l^{KJ} and C_l^{M} is smaller than the difference between C_l^{W} and C_l^{M} due to fewer assumptions that affect the accuracy of the theoretical model. This suggests that both theoretical models are accurate in a larger spectrum of angles of attack, but still, for the largest angles, both models became slightly less accurate. Due to the wide spectrum of angles in which the theory is valid, the unsteady Kutta condition will probably be valid.

Figure 8a has the same comparison but for detached flow. Here, it is evident that the flow is detached due to the drop in the lift coefficient. While the angle of attack is small, the boundary layer remains attached, but once the angle is a little higher, the flow becomes disconnected. There is a major difference between C_l^{KJ} and C_l^{M} that indicates the Kutta-Joukowski theorem is inaccurate when the flow detaches, which indicates that the unsteady Kutta condition might not be valid in this case. However, C_l^{W} and C_l^{M} are relatively close, so the comparison to

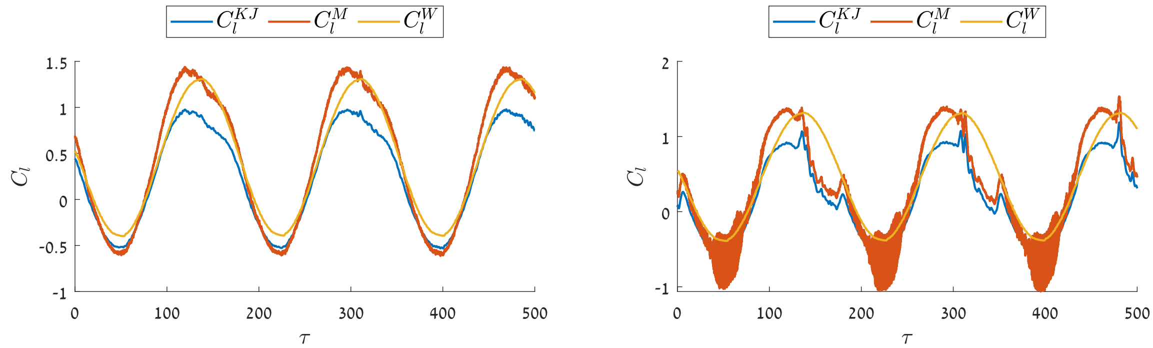

(a) Grid-generated turbulence (b) Low turbulence

Figure 8: Comparison of the calculated lift coefficients at $Re_c = 2 \times 10^5$, $\alpha = 6° \pm 12°$, and $k = 0.04$ using Kutta-Joukowski theorem, Wagner's model, and pressure measurements in attached and detached flows with (a) grid-generated turbulence and (b) low turbulence.

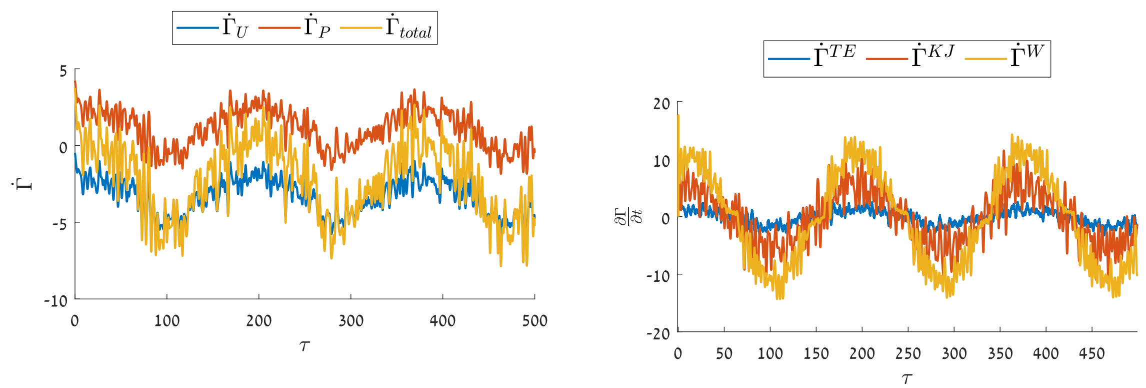

(a) Comparison of the calculated parts of Eq. (18) using pressure measurements at the trailing edge. (b) Comparison of the calculated Kutta condition.

Figure 9: Comparison of the calculated Kutta condition at $Re_c = 3 \times 10^5$, $\alpha = 0° \pm 6°$, and $k = 0.04$ using Kutta-Joukowski theorem, Wagner's model, and pressure measurements at the trailing edge in detached flows with grid-generated turbulence.

Wagner's model indicates that the unsteady Kutta condition might be valid.

Figure 8b has the same comparison as the previous two but for the bubble present. Here, it is evident that there is the LSB present due to the drastic drop in the lift coefficient, which is followed by a peak and a lot of 'noise' in the C_l^M. It can be seen that the C_l^{KJ} manages to showcase the drop in C_l^M due to the use of pressure measurements from the entire wing, which allows the theoretical formulation to consider the presence of the LSB. This is also why the drop cannot be seen in C_l^W because when using this method, the calculations are purely theoretical and do not rely on any information concerning the sudden pressure changes on the wing. This can mean that the unsteady Kutta condition may be valid when comparing the Kutta-Joukowski calculation method to the experimental results. However, if we compare the results to Wagner's model, the unsteady Kutta condition might not be valid.

In Figure 9a, the effect of the pressure fluctuations in the trailing edge in comparison to the effect of the circulation in the trailing edge on the change in vorticity over time is exhibited. We can see that the changes in circulation have a similar influence to the influence of the pressure fluctuations caused by the oscillation of the airfoil. The summation of the two describes the Kutta condition more accurately as measured at the trailing edge.

In Figure 9b we can see a comparison between the evaluated unsteady Kutta condition using Wagner's model($\dot{\Gamma}^W$), the definition of circulation (see Eq. 8) derived concerning time (calculated using Kutta-Joukowski, $\dot{\Gamma}^{KJ}$, and the measured pressure in the trailing edge as described in Eq. 18 with ($\dot{\Gamma}^{TE}$) in attached flow. It can be seen that when comparing the circulation derivative, there is a small difference between all three methods, as expected after looking at the lift coefficient comparison in this case. These differences stem from the assumption of each theoretical calculation method. Still, they are small enough to determine that the unsteady Kutta condition is valid in the case of the attached flow.

5 Conclusions

The current study investigates experimentally the unsteady phenomenon at low Reynolds numbers under transient and periodic pitching motion with a symmetric NACA 0018 airfoil geometry. The effect of reduced frequency on the characteristics of laminar separation bubbles was investigated, as well as the unsteady Kutta condition when the effect of the LSB is eliminated, i.e., with an increased turbulence level. Furthermore, the validity of thin airfoil theory and the Kutta condition [1] was examined by comparing the theoretical methods, based on circulation and thin airfoil theory, to the experimentally measured values [1–3].

Firstly, by looking at the LSB location on the wing at the tasted conditions (Reynolds number of 2×10^5), it was found that the amplitude for all reduced frequencies tested (0.04 - 0.12) is equal, meaning the reduced frequency does not affect the location of the separation of the LSB. Additionally, by looking at the normalized velocity, we can see it is compatible with the normalized LSB location in all reduced frequencies. The amplitude is the same, so the minimal and maximal location of the LSB on the wing can be achieved by normalizing the velocity. In the future, our objective is to discern the influence of each characteristic, enabling us to predict aerodynamic loads on the wing. This understanding serves as a foundation for enhancing the overall performance of the wing.

Secondly, regarding the Kutta condition, when the flow was attached, we could infer that Wagner's model and the Kutta-Joukowski theorem are less accurate for the large angles of attack. Still, comparing the results of the Kutta condition measured at the trailing edge, the one measured along the wing, and the one calculated using Wagner's model suggested that the inaccuracies are small enough, so the Kutta condition is valid. When looking at the lift coefficient comparison, it can be seen that when the flow was detached, the lift coefficient calculated using pressure measurements was similar to the one calculated using Wagner's model. Therefore, The Kutta condition may be valid in this case. However, the lift coefficient calculated using pressure measurements was incompatible with the one calculated using the Kutta-Joukowski theorem, which indicates that the Kutta condition will not be valid in this comparison.

Interestingly, when an LSB is present, there was a satisfactory match between the lift coefficient measured using pressure measurements and the one calculated using the Kutta-Joukowski theorem. This means the Kutta condition may be valid when comparing the two while the LSB is present, unlike the previous case. However, when comparing the lift coefficient measured using pressure measurements and the one calculated using Wagner's model, it is evident that the model could not represent the LSB's presence, which caused a significant difference between the two lift coefficients. This indicates that the Kutta condition will not be valid in this comparison. This comparison can reveal a fundamental understanding of what models are more accurate in estimating the aerodynamic loads in various cases. In the next step, one can locate the main inaccuracies of these theoretical models. These inaccuracies, in which the unsteady Kutta condition fails, can be used to suggest an empirical model that considers the unsteady Kutta condition. The new model can be used in various experiments aspiring to improve manoeuvrability during flight.

References

[1]W. Kutta, “Auftriebskräfte in strömenden flüssigkeiten”, Illustrierte Aeronautische Mitteilungen **6**, 133–135 (1902).

[2]N. Joukowsky, “Über die konturen der tragflächen der drachenflieger”, Zeitschrift für Flugtechnik und Motorluftschiffahrt **1**, 281–285 (1910).

[3]H. Wagner, “Über die entstehung des dynamischen auftriebes von tragflügeln”, Z. Angew. Math. Mech. **5**, 17–35 (1924).

[4]C. Strangfeld, H Müller-Vahl, C. Nayeri, C. Paschereit, and D Greenblatt, “Airfoil in a high amplitude oscillating stream”, Journal of Fluid Mechanics **793**, 79–108 (2016).

[5]G. Sedky, A. Gementzopoulos, I. Andreu-Angulo, F. D. Lagor, and A. R. Jones, “Physics of gust response mitigation in open-loop pitching manoeuvres”, Journal of Fluid Mechanics **944**, A38 (2022).

[6]T. Theodorsen, “General general theory of aerodynamic instability and the mechanism of”, Annual Report of the National Advisory Committee for Aeronautics **268**, 413 (1935).

[7]T. Lee and P. Gerontakos, “Investigation of flow over an oscillating airfoil”, Journal of Fluid Mechanics **512**, 313–341 (2004).

[8]B. Turhan, Z. Wang, and I. Gursul, “Coherence of unsteady wake of periodically plunging airfoil”, Journal of Fluid Mechanics **938** (2022).

[9]W. J. McCroskey, *The phenomenon of dynamic stall. NASA Tech. Rep.* 81264 (1981).

[10]T. Zhou, Y. Sun, R. Fattah, X. Zhang, and X. Huang, “An experimental study of trailing edge noise from a pitching airfoil”, The Journal of the Acoustical Society of America **145**, 2009–2021 (2019).

[11]D. Raus, B. Cotté, R. Monchaux, E. Jondeau, Souchotte, and M. Roger, “Experimental study of the dynamic stall noise on an oscillating airfoil”, Journal of Sound and Vibration **537**, 117144 (2022).

[12]Y. D. Mayer, B Zang, and M. Azarpeyvand, “Aeroacoustic investigation of an oscillating airfoil in the pre-and post-stall regime”, Aerospace Science and Technology **103**, 105880 (2020).

[13]R. L. Bisplinghoff, H. Ashley, and R. L. Halfman, *Aeroelasticity* (Courier Corporation, 2013).

[14]M. R. Catlett, “Investigation into the unsteady response of airfoils due to small-scale motion”, PhD thesis (University of Maryland, College Park, 2020).

[15]D. Raus, B. Cotté, R. Monchaux, E. Jondeau, P. Souchotte, and M. Roger, “Experimental study of the dynamic stall noise on an oscillating airfoil”, Journal of Sound and Vibration **537**, 117144 (2022).

[16]J. Kiefer, C. E. Brunner, M. O. Hansen, and M. Hultmark, “Dynamic stall at high reynolds numbers induced by ramp-type pitching motions”, Journal of Fluid Mechanics **938**, A10 (2022).

[17]D.-H. Kim and J.-W. Chang, “Unsteady boundary layer for a pitching airfoil at low reynolds numbers”, Journal of Mechanical Science and Technology **24**, 429–440 (2010).

[18]K. Rogowski, G. Królak, and G. Bangga, “Numerical study on the aerodynamic characteristics of the naca 0018 airfoil at low reynolds number for darrieus wind turbines using the transition sst model”, Processes **9**, 477 (2021).

[19]M. Kaushik, *Theoretical and experimental aerodynamics* (Springer, 2019).

[20]I. E. Garrick, "On some reciprocal relations in the theory of nonstationary flows", (1938).

[21]A. S. Rezaei, *Reduced-order modeling of unsteady aerodynamics: theoretical and computational approaches* (University of California, Irvine, 2019).

[22]T. H. von Kárman and W. R. Sears, "Airfoil theory for non-uniform motion", Journal of the Aeronautical Sciences **5**, 379–390 (1938).

[23]N. H. Kemp, "On the lift and circulation of airfoils in some unsteady-flow problems", Journal of the Aeronautical Sciences **19**, 713–714 (1952).

[24]P. Walker, "Experiments on the growth of circulation about a wing", Techn. Rep. Aeron. Res. Committee (1931).

[25]R. L. Halfman, *Experimental aerodynamic derivatives of a sinusoidally oscillating airfoil in two-dimensional flow*, *NACA Tech. Rep.* 2465 (1951).

[26]C.-Y. Chow and M.-K. Huang, "The initial lift and drag of an impulsively started airfoil of finite thickness", Journal of Fluid Mechanics **118**, 393–409 (1982).

[27]J. Graham, "The lift on an aerofoil in starting flow", Journal of Fluid Mechanics **133**, 413–425 (1983).

[28]C. P. Ford and H. Babinsky, "Lift and the leading-edge vortex", Journal of Fluid Mechanics **720**, 280–313 (2013).

[29]J. Li and Z.-N. Wu, "Unsteady lift for the wagner problem in the presence of additional leading/trailing edge vortices", Journal of Fluid Mechanics **769**, 182–217 (2015).

[30]R Jackson, J. Graham, and D. Maull, "The lift on a wing in a turbulent flow", Aeronautical Quarterly **24**, 155–166 (1973).

[31]G. L. Commerford and F. O. Carta, "Unsteady aerodynamic response of a two-dimensional airfoil at high reduced frequency", AIAA Journal **12**, 43–48 (1974).

[32]U. Cordes, G. Kampers, T. Meißner, C. Tropea, J. Peinke, and M. Hölling, "Note on the limitations of the theodorsen and sears functions", Journal of Fluid Mechanics **811** (2017).

[33]A. G. Rainey, *Measurement of aerodynamic forces for various mean angles of attack on an airfoil oscillating in pitch and on two finite-span wings oscillating in bending with emphasis on damping in the stall*, *NACA Tech. Rep.* 1305 (1957).

[34]S. Ōtomo, S. Henne, K. Mulleners, K. Ramesh, and I. M. Viola, "Unsteady lift on a high-amplitude pitching aerofoil", Experiments in Fluids **62**, 1–18 (2021).

[35]D. R. Williams, F. Reißner, D. Greenblatt, H. F. Müller-Vahl, and C. Strangfeld, "Modeling lift hysteresis on pitching airfoils with a modified goman–khrabrov model", AIAA Journal **55**, 403–409 (2017).

[36]S. J. Schreck, W. E. Faller, and H. E. Helin, "Pitch rate and reynolds number effects on unsteady boundary-layer transition and separation", Journal of Aircraft **35**, 46–52 (1998).

[37]M. Soltani and A Bakhshalipour, "Effect of amplitude and mean angle-of-attack on the boundary layer of an oscillating aerofoil", The Aeronautical Journal **112**, 705–713 (2008).

[38]H. P. Horton, "Laminar separation bubbles in two and three dimensional incompressible flow.", PhD thesis (Queen Mary University of London, 1968).

[39]I. Tani, “Low-speed flows involving bubble separations”, Progress in Aerospace Sciences **5**, 70–103 (1964).

[40]D. W. Wynnychuk and S. Yarusevych, “Characterization of laminar separation bubbles using infrared thermography”, AIAA Journal **58**, 2831–2843 (2020).

[41]A. R. Lambert and S. Yarusevych, “Characterization of vortex dynamics in a laminar separation bubble”, AIAA Journal **55**, 2664–2675 (2017).

[42]S. Yarusevych, P. E. Sullivan, and J. G. Kawall, “On vortex shedding from an airfoil in low-reynolds-number flows”, Journal of Fluid Mechanics **632**, 245–271 (2009).

[43]M. O’meara and T. J. Mueller, “Laminar separation bubble characteristics on an airfoil at low reynolds numbers”, AIAA journal **25**, 1033–1041 (1987).

[44]S. Burgmann and W Schröder, “Investigation of the vortex induced unsteadiness of a separation bubble via time-resolved and scanning piv measurements”, Experiments in fluids **45**, 675–691 (2008).

[45]S. Hosseinverdi and H. F. Fasel, “Numerical investigation of laminar–turbulent transition in laminar separation bubbles: the effect of free-stream turbulence”, Journal of Fluid Mechanics **858**, 714–759 (2019).

[46]M Pascazio, J Autric, D Favier, and C Maresca, “Unsteady boundary-layer measurement on oscillating airfoils-transition and separation phenomena in pitching motion”, in 34th aerospace sciences meeting and exhibit (1996), p. 35.

[47]T Lee and S Basu, “Measurement of unsteady boundary layer developed on an oscillating airfoil using multiple hot-film sensors”, Experiments in Fluids **25**, 108–117 (1998).

[48]L. Ericsson and J. Reding, “Fluid mechanics of dynamic stall part i. unsteady flow concepts”, Journal of fluids and structures **2**, 1–33 (1988).

[49]A Nati, R De Kat, F. Scarano, and B. Van Oudheusden, “Dynamic pitching effect on a laminar separation bubble”, Experiments in fluids **56**, 1–17 (2015).

[50]A. Grille Guerra, C. Mertens, J. Little, and B. van Oudheusden, “Experimental characterization of an unsteady laminar separation bubble on a pitching wing”, Experiments in Fluids **64**, 16 (2023).

[51]X. Xia and K. Mohseni, “Unsteady aerodynamics and vortex-sheet formation of a two-dimensional airfoil”, Journal of Fluid Mechanics **830**, 439–478 (2017).

[52]W. Zhu, M. H. McCrink, J. P. Bons, and J. W. Gregory, “The unsteady kutta condition on an airfoil in a surging flow”, Journal of Fluid Mechanics **893** (2020).

[53]J. Giesing, “Vorticity and kutta condition for unsteady multienergy flows”, (1969).

[54]S. Fleeter, “Trailing edge conditions for unsteady flows at high reduced frequency”, AIAA Journal **18**, 497–503 (1980).

[55]B. Satyanarayana and S. Davis, “Experimental studies of unsteady trailing-edge conditions”, AIAA Journal **16**, 125–129 (1978).

[56]S. T. Dawson and S. L. Brunton, “Improved approximations to wagner function using sparse identification of nonlinear dynamics”, AIAA Journal **60**, 1691–1707 (2022).

[57]R. T. Jones, *Operational treatment of the nonuniform-lift theory in airplane dynamics*, *NACA Tech. Rep.* 667 (1938).

[58]W. P. Jones, "Aerodynamic forces on wings in non-uniform motion", ARC Technical Report, R. & M. No. 2117 (1945).

[59]S. L. Brunton and C. W. Rowley, "Empirical state-space representations for theodorsen's lift model", Journal of Fluids and Structures **38**, 174–186 (2013).

[60]J. Anderson, *Ebook: fundamentals of aerodynamics (si units)* (McGraw hill, 2011).

[61]W. Sears, "Some recent developments in airfoil theory", Journal of the Aeronautical Sciences **23**, 490–499 (1956).

[62]H. Taha and A. S. Rezaei, "Viscous extension of potential-flow unsteady aerodynamics: the lift frequency response problem", Journal of Fluid Mechanics **868**, 141–175 (2019).

[63]J. Preston, *The approximate calculation of the lift of symmetrical aerofoils taking account of the boundary layer, with application to control problems* (HM Stationery Office, 1943).

[64]D. Spence, "Prediction of the characteristics of two-dimensional airfoils", Journal of the Aeronautical Sciences **21**, 577–587 (1954).

[65]J. Katz and A. Plotkin, *Low-speed aerodynamics*, Vol. 13 (Cambridge university press, 2001).

[66]W. Timmer, "Two-dimensional low-reynolds number wind tunnel results for airfoil naca 0018", Wind Engineering **32**, 525–537 (2008).

[67]G. B. McCullough and D. E. Gault, *Examples of three representative types of airfoil-section stall at low speed*, *NACA Tech. Rep.* 2505 (1951).

[68]D.-H. Kim, J.-W. Chang, and H.-B. Kim, "Aerodynamic characteristics of a pitching airfoil through pressure-distortion correction in pneumatic tubing", Journal of Aircraft **50**, 590–598 (2013).

[69]H. F. Müller-Vahl, "Wind turbine blade dynamic stall and its control", PhD thesis (Technion, Israel Institute of Technology and Technische Universität Berlin, 2015).

[70]M. S. Istvan, J. W. Kurelek, and S. Yarusevych, "Turbulence intensity effects on laminar separation bubbles formed over an airfoil", AIAA Journal **56**, 1335–1347 (2018).

[71]M. Drela, "Xfoil: an analysis and design system for low reynolds number airfoils", in Low reynolds number aerodynamics: proceedings of the conference notre dame, indiana, usa, 5–7 june 1989 (Springer, 1989), pp. 1–12.

[72]M. Gaster, *The structure and behaviour of laminar separation bubbles* (Citeseer, 1967).

[73]A. S. Rezaei and H. Taha, "Circulation dynamics of small-amplitude pitching airfoil undergoing laminar-to-turbulent transition", Journal of Fluids and Structures **100**, 103177 (2021).